J|A|C|S ARTICLES

Published on Web 06/10/2010

Orientation, Dynamics, and Lipid Interaction of an Antimicrobial Arylamide Investigated by ^{19}F and ^{31}P Solid-State NMR Spectroscopy

Yongchao Su,[†] William F. DeGrado,[‡] and Mei Hong*[,†]

Department of Chemistry, Iowa State University, Ames, Iowa 50011 and Department of Biochemistry and Biophysics, University of Pennsylvania, Philadelphia, Pennsylvania 19104-6059

Received April 29, 2010; E-mail: mhong@iastate.edu

Abstract: A number of arylamides have been synthesized and found to exhibit potent antimicrobial activities against a broad spectrum of Gram-positive and Gram-negative bacteria while exhibiting low toxicity toward eukaryotic cells. These facially amphiphilic foldamers have a relatively rigid intramolecular hydrogen-bonded arylamide as a framework, which places trifluormethyl versus positively charged amino and guanidino groups along opposite faces of the elongated molecule, facilitating interactions with lipid membranes. To better understand the mechanism of action of these antimicrobial foldamers, we have investigated the lipid interaction, depth of insertion, orientation, and dynamics of an arylamide, PMX30016, using ^{31}P and ^{19}F solid-state NMR spectroscopy. Static ^{31}P NMR line shapes of lipid membranes with a range of compositions indicate that PMX30016 does not disrupt the lamellar order of the lipid bilayer but perturbs the lipid headgroup conformation. This headgroup perturbation, manifested as systematic ^{31}P chemical shift anisotropy increases, is consistent with the well documented "electrometer" effect of lipid membranes in response to the addition of positive charges to membrane surfaces. Paramagnetic relaxation enhancement experiments indicate that the arylamide inserts into the membrane−water interface, just below the headgroup region. Measurement of $^{19}F-^{19}F$ dipolar couplings within each CF_3 moiety revealed that PMX30016 is oriented with the molecular plane 20° and 30° from the membrane normal of neutral and anionic bilayers, respectively, and the long molecular axis lies parallel to the membrane plane. Thus, this arylamide inserts into the bilayer in a knife-like fashion, consistent with previous vibrational spectroscopy results. Moreover, ^{19}F NMR line shapes indicate that this molecular knife undergoes fast uniaxial rotation around the bilayer normal. These results suggest that antimicrobial arylamides destabilize anionic lipid membranes primarily by altering the membrane electric potential profile, and the spinning molecular knife may additionally create transient defects in the lipid membrane. Compared to typical antimicrobial peptides, this arylamide has more subtle effects on and is less disruptive of the structure of lipid bilayers.

Introduction

Antimicrobial peptides (AMPs) have attracted much attention in the past two decades as potentially alternative antibiotics against drug-resistant bacteria.[1] Many naturally occurring AMPs have been discovered that possess broad-spectrum and potent antimicrobial activities against many bacteria. However, despite the large number of AMPs studied, therapeutic applications have been limited by their relatively large size, toxicity, and difficulties associated with large-scale synthesis of these molecules.[1] Thus, it is important to design smaller and more structurally robust synthetic antimicrobial molecules with the essential structural requirements for potent antimicrobial activity and low toxicity. It is by now well-known that AMP activities often correlate with their amphiphilic structures and high cationic charge densities, which enable them to selectively target and disrupt the negatively charged lipid membranes of microbial cells.[2] Based on these considerations, short sequences of synthetic antimicrobial foldamers have been designed that contain arylamide,[3] phenylene ethynylene,[4,5] polynorbornene,[6,7] and polymethacrylate[8] backbones. The arylamide series has been particularly well studied. The arylamide backbone is decorated with basic guanidinium side chains and hydrophobic moieties, and the molecules are conformationally rigid by virtue of thioether-based intramolecular hydrogen bonds and amide

[†] Iowa State University.
[‡] University of Pennsylvania.

(1) Zasloff, M. *Nature* **2002**, 389–395.
(2) Epand, R. M.; Vogel, H. J. *Biochim. Biophys. Acta* **1999**, *1462*, 11–28.
(3) Tew, G. N.; Liu, D.; Chen, B.; Doerksen, R. J.; Kaplan, J.; Carroll, P. J.; Klein, M. L.; DeGrado, W. F. *Proc. Natl. Acad. Sci. U.S.A.* **2002**, *99*, 5110–5114.
(4) Tew, G. N.; Clements, D.; Tang, H.; Arnt, L.; Scott, R. W. *Biochim. Biophys. Acta* **2006**, *1758*, 1387–1392.
(5) Yang, L.; Gordon, V. D.; Trinkle, D. R.; Schmidt, N. W.; Davis, M. A.; DeVries, C.; Som, A.; Cronan, J. E.; Tew, G. N.; Wong, G. C. *Proc. Natl. Acad. Sci. U.S.A.* **2008**, *105*, 20595–20600.
(6) Gabriel, G. J.; Pool, J. G.; Som, A.; Dabkowski, J. M.; Coughlin, E. B.; Muthukumar, M.; Tew, G. N. *Langmuir* **2008**, *24*, 12489–12495.
(7) Som, A.; Vemparala, S.; Ivanov, I.; Tew, G. N. *Biopolymers* **2008**, *90*, 83–93.
(8) Kuroda, K.; DeGrado, W. F. *J. Am. Chem. Soc.* **2005**, *127*, 4128–4129.

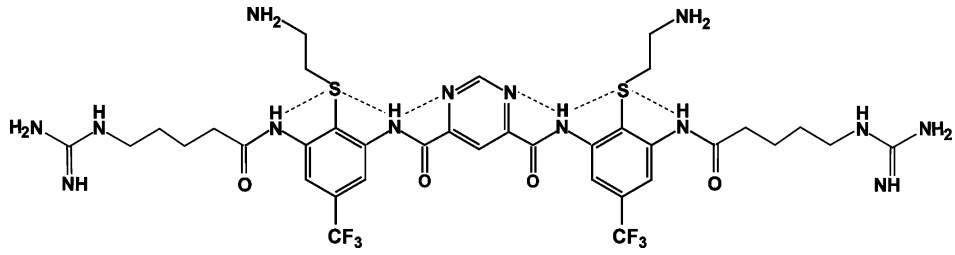

Figure 1. Molecular structure of PMX30016. Dash lines indicate the intramolecular hydrogen bonds.

groups.[9,10] Structure−activity relationship studies revealed that the amphiphilicity and conformational rigidity of these arylamide foldamers are essential for their high antimicrobial potency and low toxicity, and members of this class of foldamers have been found to have low minimum inhibitory concentrations (MICs) but high EC_{50} or HC_{50} values toward eukaryotic cells.[9,11]

While the antimicrobial activities of arylamide foldamers have been extensively studied, the physical mechanism of their interaction with the lipid membrane is still not well understood. Determining the three-dimensional structure and topology of these antimicrobial molecules in the lipid bilayer is essential for elucidating their mechanisms of action. So far, sum frequency generation (SFG) vibrational spectroscopy[12,13] and molecular dynamics (MD) simulations[14,15] have been used to deduce the topological structure and dynamics of the arylamides in the membrane. These studies suggest that the arylamide oligomers insert into the membrane perpendicular to the bilayer surface and do not cause the formation of water pores in the membrane. However, high-resolution orientational constraints, depth of insertion, and the mobility of the arylamides have not been reported.

The chemical structure of one of the arylamide foldamers, PMX30016, is shown in Figure 1. The molecule consists of a central pyrimidine ring flanked by two phenylene diamine units. A thioether moiety allows the attachment of basic groups and forms intramolecular hydrogen bonds with neighboring amides. The phenylene diamine rings are also decorated with a trifluoromethyl group and a terminal guanidine-pentanoyl side chain that increases the positive charge density of the molecule. PMX30016 was found to have excellent therapeutic indices: its MICs are 0.1 μM against Gram-negative *E. coli* and 0.2 μM against Gram-positive tetracyclin- and streptomycin-resistant *S. aureus*, and its HC_{50} against red blood cells is 440 μM.[9,10]

In this work, we use ^{31}P and ^{19}F solid-state NMR spectroscopy to determine the lipid interaction and membrane topology of this arylamide foldamer in lipid bilayers of varying compositions. ^{31}P NMR is a sensitive probe of the membrane morphology and disorder induced by antimicrobial molecules.[16−18] ^{19}F NMR is a highly sensitive and background-free indicator of membrane-active molecules and has been used extensively for determining the orientation[19,20] and quaternary structure[21−23] of oligomeric membrane peptides and proteins. While the three ^{19}F spins of a trifluoromethyl group are chemically equivalent, dipolar couplings among the three spins are observable and depend on the orientation of the C−CF_3 bond with respect to the membrane normal.[24] We used a simple 2D dipolar-chemical-shift correlation technique to resolve the orientation-dependent ^{19}F−^{19}F dipolar coupling from the ^{19}F chemical shift pattern. Combined with paramagnetic relaxation enhancement experiments, we have determined both the orientation and the depth of insertion of PMX30016 in lipid bilayers and propose its membrane disruptive mechanism.

Materials and Methods

Lipids and Arylamide Compound. All lipids, including 1-palmitoyl-2-oleoyl-*sn*-glycero-3-phosphatidylcholine (POPC), 1-palmitoyl-2-oleoyl-*sn*-glycero-3-phosphatidylglycerol (POPG), 1-palmitoyl-2-oleoyl-*sn*-glycero-3-phosphatidylserine (POPS), 1,2-dimyristoyl-*sn*-glycero-3-phosphochloline (DMPC), 1,2-dimyristoyl-*sn*-glycero-3-phosphatidylglycerol (DMPG), dihexylphosphatidylcholine (6-O-PC), and cholesterol were purchased from Avanti Polar Lipids (Alabaster, AL) and used without further purification. PMX30016 was synthesized by PolyMedix (Radnor, PA).

Membrane Sample Preparation. Glass-plate oriented lipid membranes containing varying concentrations of PMX30016 were prepared using a naphthalene-incorporated method.[25] After codissolving PMX30016, lipids, and naphthalene at desired molar ratios in MeOH/$CHCl_3$ (1:2, v/v), the solution was deposited dropwise onto 6 × 12 mm^2 glass plates (Marienfeld, Germany). After drying overnight in a lyophilizer, the lipid films were hydrated first by directly applying 5 μL of water on each plate, followed by incubation in a 97% humidity chamber containing saturated K_2SO_4 solution at 20 °C for 4−5 days. Finally, the glass plates were stacked and wrapped with parafilm for static ^{31}P NMR experiments. We prepared four membrane series with different lipid compositions: POPE/POPG (3:1), POPC/POPG (3:1), POPC/POPS (4.5:1), and POPC/POPS/cholesterol (4.5:1:2.4).

(9) Tew, G. N.; Scott, R. W.; Klein, M. L.; DeGrado, W. F. *Acc. Chem. Res.* **2010**, *43*, 30–39.
(10) Choi, S.; Isaacs, A.; Clements, D.; Liu, D.; Kim, H.; Scott, R. W.; Winkler, J. D.; DeGrado, W. F. *Proc. Natl. Acad. Sci. U.S.A.* **2009**, *106*, 6968–6973.
(11) Scott, R. W.; DeGrado, W. F.; Tew, G. N. *Curr. Opin. Biotechnol.* **2008**, *19*, 620–627.
(12) Chen, X.; Tang, H.; Even, M. A.; Wang, J.; Tew, G. N.; Chen, Z. *J. Am. Chem. Soc.* **2006**, *128*, 2711–2714.
(13) Avery, C. W.; Som, A.; Xu, Y.; Tew, G. N.; Chen, Z. *Anal. Chem.* **2009**, *81*, 8365–8372.
(14) Lopez, C. F.; Nielsen, S. O.; Srinivas, G.; DeGrado, W. F.; Klein, M. L. *J. Chem. Theory. Comput.* **2006**, *2*, 649–655.
(15) Liu, D.; Choi, S.; Chen, B.; Doerksen, R. J.; Clements, D. J.; Winkler, J. D.; Klein, M. L.; DeGrado, W. F. *Angew. Chem., Int. Ed.* **2004**, *43*, 1033.
(16) Buffy, J. J.; McCormick, M. J.; Wi, S.; Waring, A. J.; Lehrer, R. I.; Hong, M. *Biochemistry* **2004**, *43*, 9800–9812.
(17) Doherty, T.; Waring, A. J.; Hong, M. *Biochim. Biophys. Acta* **2006**, 1285–1291.
(18) Mani, R.; Buffy, J. J.; Waring, A. J.; Lehrer, R. I.; Hong, M. *Biochemistry* **2004**, *43*, 13839–13848.
(19) Ulrich, A. S. *Prog. Nucl. Magn. Reson. Spectrosc.* **2005**, 1–21.
(20) Glaser, R. W.; Sachse, C.; Dürr, U. H.; Wadhwani, P.; Afonin, S.; Strandberg, E.; Ulrich, A. S. *Biophys. J.* **2005**, *88*, 3392–3397.
(21) Luo, W.; Hong, M. *J. Am. Chem. Soc.* **2006**, 7242–7251.
(22) Luo, W.; Mani, R.; Hong, M. *J. Phys. Chem.* **2007**, *111*, 10825–10832.
(23) Hong, M. *J. Phys. Chem. B.* **2007**, 10340–10351.
(24) Grage, S. L.; Ulrich, A. S. *J. Magn. Reson.* **2000**, 81–88.
(25) Hallock, K. J.; Henzler-Wildman, K. A.; Lee, D. K.; Ramamoorthy, A. *Biophys. J.* **2002**, 2499–2503.

The bicelle samples for orientation determination were prepared using published protocols.[26] Briefly, the zwitterionic lipid DMPC was mixed with the ether lipid 6-O-PC at a DMPC/6-O-PC molar ratio of $q = 3.2$ to a total lipid concentration of 35% (w/v) in pH 7.0 phosphate buffer. The mixture was vortexed, heated to 42 °C, and cooled to 5 °C until a clear, homogeneous, and viscous solution was obtained. Static ^{31}P NMR spectra confirmed that the lipid mixture was well aligned in the membrane with the bilayer normal perpendicular to the magnetic field at 306 K. PMX30016 was added to the bicelle solution to a drug/lipid molar ratio of 1:15 and then subjected to another round of vortexing as well as heating and cooling cycles, and the alignment of the resulting bicelle was again checked by ^{31}P NMR.

Unoriented PMX30016-containing lipid membranes were prepared by mixing PMX30016 with DMPC/DMPG (3:1) vesicles at a molar ratio of 1:15. The solution was incubated overnight and then spun down to obtain a hydrated membrane pellet. UV−vis spectroscopy showed that >96% of PMX30016 was bound to the lipids.

For paramagnet relaxation enhancement (PRE) experiments, 5 mol % Mn^{2+} relative to the total molar amount of lipids were added to hydrated DMPC/DMPG vesicles containing PMX30016. In general, Mn^{2+} ions added to a lipid vesicle solution cannot cross a lipid bilayer that is free of any defects or pores. Thus, all Mn^{2+} ions should be distributed on the outer surface of the bilayer, as demonstrated by NMR.[27] However, freeze−thawing a one-sided Mn^{2+}-bound membrane sample redistributes the ions to both surfaces of the membrane due to the fragmentation of the bilayer by ice. We prepared both one-sided and two-sided Mn^{2+}-bound membrane samples containing PMX30016 to assess the depth and polarity of insertion of the arylamide compound.

Solid-State NMR Experiments. All solid-state NMR experiments were carried out on a Bruker DSX-400 spectrometer (Karlsruhe, Germany) operating at a resonance frequency of 376.8 MHz for ^{19}F and 162.1 MHz for ^{31}P. Typical radio frequency (rf) pulse lengths were 5 μs for ^{1}H and ^{31}P and 6 μs for ^{19}F. ^{31}P chemical shifts were referenced to the liquid phosphoric acid peak at 0 ppm for the oriented membrane experiments and to the isotropic signal of hydroxyapatite at +2.73 ppm on the phosphoric acid scale for unoriented membrane experiments. The ^{19}F chemical shifts were referenced to the Teflon isotropic ^{19}F signal at −122 ppm.

A double-resonance probe equipped with a custom-designed 6 × 12 × 5 mm^3 rectangular coil was used for the ^{31}P NMR experiments on glass-plate oriented samples. The samples were positioned in the magnet with the alignment axis parallel to the magnetic field. The ^{31}P spectra were measured at 296 K by single pulse excitation. A $^{1}H/^{19}F/X$ magic-angle-spinning (MAS) probe was used for all ^{19}F experiments. Static 1D ^{31}P and ^{19}F spectra of bicelle samples were measured at 306 K, at which the bicelle maintains good magnetic alignment. A 2D ^{1}H-decoupled correlation experiment (Figure 5a) was implemented to correlate the $^{19}F-^{19}F$ dipolar coupling with the ^{19}F chemical shift anisotropy. A dwell time of 20 μs and a total t_1 evolution time of 6.4 ms were used.

Orientation Calculation and ^{19}F NMR Line Shape Analysis. The two C−CF_3 bonds lie mostly in the molecular plane formed by the centers of the three aromatic rings (Figure 6a). The angle between the C−CF_3 bond and the long molecular axis, which is defined as the vector connecting the two carbons ortho to the nitrogen atoms of the pyrimidine ring, is 72°.

For orientation calculations, we defined a molecule-fixed frame where the x-axis is the long molecular axis described above, the y-axis lies in the plane of the central aromatic ring, perpendicular to the ortho C−C vector, and the z-axis is perpendicular to the ring (Figure 6a). The direction of the bilayer normal relative to the molecule is defined by a tilt angle τ from the z-axis and a rotation angle ρ between the x-axis and the projection of the bilayer normal onto the $x-y$ plane. By rotating the bilayer normal through all combinations of (τ, ρ) from 0° to 360°, we can obtain the corresponding C−CF_3 bond orientations to the bilayer normal and thus calculate the $^{19}F-^{19}F$ dipolar couplings as averaged by the CF_3 rotation to be along the C−CF_3 bond.

The chemical shift anisotropy (CSA) tensor is defined by three principal values, δ_{xx},δ_{yy},δ_{zz}, whose average is the isotropic shift $\delta_{iso} = (\delta_{xx} + \delta_{yy} + \delta_{zz})/3$. The anisotropy parameter δ is defined as $\delta = \delta_{zz} - \delta_{iso}$, and the asymmetry parameter η is defined as $\eta = (\delta_{yy} - \delta_{xx})/(\delta_{zz} - \delta_{iso})$. The δ_{yy} principal value is the closest to the isotropic chemical shift while δ_{zz} is the furthest. Powder patterns with $\eta = 0$ due to identical δ_{yy} and δ_{xx} frequencies are called uniaxial powder patterns. Another indicator of the size of the CSA is the span $\Delta\sigma = \delta_{zz} - \delta_{xx}$. For $\eta = 0$ CSA patterns, which are observed for all uniaxially diffusive molecules in lipid bilayers, the frequency position $\delta_{xx} = \delta_{yy}$ is called the 90° edge since they result from molecules whose bilayer normal is perpendicular to the magnetic field, while the δ_{zz} frequency is called the 0° edge.

Results

The PMX30016 structure has a 2-fold symmetry with respect to the central ring (Figure 1). The pyrimidine-4,6-dicarboxylic center is connected to a *m*-phenylenediamine group on each side. A CF_3 group and a thioether group are attached to each *m*-phenylenediamine to increase the amphiphilicity of the molecule. The molecule is terminated at the two ends by a hydrophilic guanidine-pentanoyl side chain. The aromatic rings, amide groups, and hydrogen bonds create a highly rigid molecule, which was found to be important for antimicrobial potency and selectivity.[10] The compound has a molecular weight of 1063 Da, which is smaller than that of most antimicrobial peptides, which have molecular weights of 2−5 kDa.

Membrane Perturbation by PMX30016. Static ^{31}P NMR line shapes of aligned lipid membranes are sensitive reporters of the types of lipid morphology caused by antimicrobial molecules. Both the anisotropic frequency and the intensity distribution reflect the membrane morphology and the lipid headgroup packing. Lamellar bilayers aligned with the bilayer normal parallel to the magnetic field exhibit a single narrow peak at ∼30 ppm. Unoriented bilayers show a broad powder pattern with maximum intensity at approximately −12 ppm. Isotropic vesicles and micelles give a sharp isotropic signal near 0 ppm (Figure 2a). Membranes whose orientational order is perturbed by antimicrobial peptides often exhibit residual powder patterns and intensities at the 90° edge. Thus the area fraction of the disordered region reflects the extent of the membrane disruption.[16,18]

Figure 2b shows the static ^{31}P spectra of four series of oriented membranes in the presence of varying concentrations of PMX30016. Three series combine a zwitterionic lipid (POPE or POPC) with a negatively charged lipid (POPG or POPS) to mimic the bacterial cell membrane composition, while the fourth series contains cholesterol along with POPC and POPS to mimic the eukaryotic membrane composition. Interestingly, we did not observe any significant residual powder patterns or isotropic intensities in these spectra up to a peptide molar concentration of 16%. The fractional disorder is 20−35% at 8% PMX30016, which is small compared to most antimicrobial peptides.[16,18] Thus, PMX30016 does not disrupt the overall lamellar morphology of the bilayer. However, in all four series the 0° ^{31}P peak shifted downfield (to larger chemical shifts) with increasing concentrations of PMX30016, indicating that the electronic environment of the ^{31}P was altered by the drug. Using the difference between the 0° and 90° edges of the powder pattern as an indicator of the magnitude of the ^{31}P CSA, we found that

(26) De Angelis, A.; Opella, S. J. *Nat. Protoc.* **2007**, *2*, 2332–2338.
(27) Su, Y.; Mani, R.; Hong, M. *J. Am. Chem. Soc.* **2008**, *130*, 8856–8864.

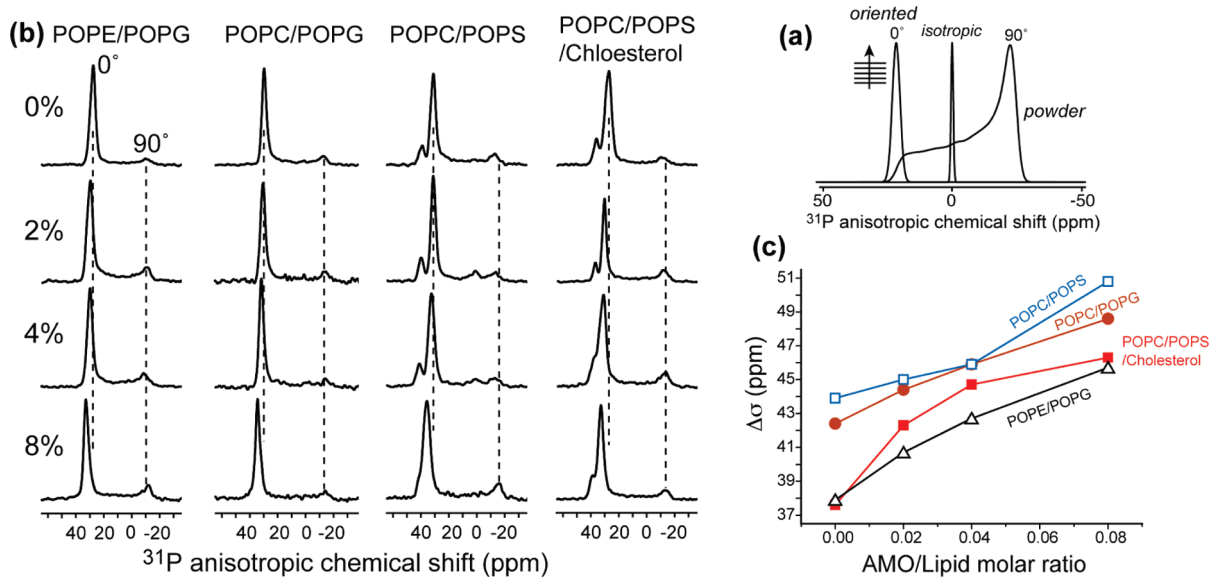

Figure 2. (a) Static ^{31}P line shapes of representative membrane morphologies. (b) Static ^{31}P spectra of oriented lipid membranes of different compositions in the presence of PMX30016 at 296 K. The PMX30016 molar concentrations are 0%, 2%, 4%, and 8% from top to bottom. The membrane compositions are POPE/POPG, POPC/POPG (brown), POPC/POPS (blue), and POPC/POPS/cholesterol (red). (c)^{31}P chemical shift anisotropy (CSA) change of different lipid membranes as a function of PMX30016 concentration.

the span increased by 6.2−8.7 ppm, or 15−23%, for the four membrane series between 0 and 8% arylamide (Figure 2c). Upon addition of 16% PMX30016, the most bacteria-mimetic membrane, POPE/POPG, showed a span increase of 9.3 ppm (26%), while the most eukaryote-mimetic POPC/POPS/cholesterol membrane exhibited a span increase of 13.2 ppm (32%) (data not shown).

Binding of PMX30016 to the Membrane−Water Interface. To determine the depth of insertion of PMX30016 in lipid membranes, we carried out a paramagnetic resonance enhancement (PRE) experiment using Mn^{2+} ions. Mn^{2+} ions bind to the surfaces of lipid bilayers and enhance the T_2 relaxation rates of nuclear spins in a distance-dependent fashion. The closer the nuclear spins to the paramagnetic center, the broader and lower the signal intensities.[28] The ratio of the peak height in the presence of Mn^{2+} to the full intensity in the absence of Mn^{2+} reflects the distance of the nuclear spins to the paramagnetic ions on the membrane surface. By comparing the PRE effect of the peptide signals with that of lipid functional groups, whose depths are known,[29] we can thus determine the insertion depth of PMX30016.

Figure 3a shows the single-pulse ^{31}P spectra of the DMPC/DMPG bilayer and ^{19}F spectra of PMX30016. Three spectra, without Mn^{2+}, with Mn^{2+} on the outer surface of the bilayer, and with Mn^{2+} on both surfaces of the bilayer, are compared. The one-sided Mn^{2+} sample reduced the ^{31}P intensity to 26% and the ^{19}F signal of the arylamide to a similar level of 29%. The addition of Mn^{2+} to both surfaces of the bilayer further decreased the ^{31}P and ^{19}F signals. Again, the residual ^{19}F signal height (12%) is larger than the residual ^{31}P signal (8%), indicating that the CF_3 groups are buried more deeply than the phosphate group. The lower NMR signals of the one-sided Mn^{2+} sample compared to the two-sided Mn^{2+} sample indicates that the arylamide, just like the lipid, is bound to both leaflets of the bilayer rather than to only the outer leaflet, since the distance

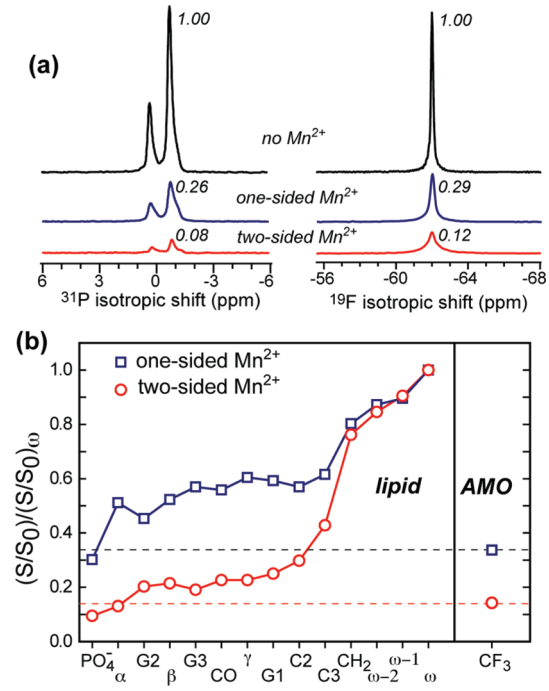

Figure 3. Depth of insertion of PMX30016 in lipid membranes from Mn^{2+} paramagnetic relaxation enhancement experiments. (a) ^{31}P and ^{19}F MAS spectra of PMX30016-containing DMPC/DMPG (3:1) bilayers without Mn^{2+} (black), with Mn^{2+} on the outer membrane surface (blue), and with Mn^{2+} on both membrane surfaces. The intensities normalized to the Mn^{2+}-free samples are indicated. (b) PRE effects of PMX30016 in DMPC/DMPG (3:1) bilayers containing 5% Mn^{2+}. The ratio of the lipid ^{13}C intensities (not shown) between the Mn^{2+}-containing sample (S) and a Mn^{2+}-free control sample (S_0) is S/S_0. This dephasing value was further normalized to the S/S_0 of the acyl-chain terminal methyl group ω. The ^{19}F intensity of PMX30016 is comparable to the glycerol and headgroup carbons, indicating that PMX30016 is associated to the membrane−water interface, close to the surface water.

from the outer leaflet to the inner surface of the membrane is sufficiently large that purely outer-leaflet bound molecules would not experience sufficient PRE effect from Mn^{2+} ions on the inner

(28) Buffy, J. J.; Hong, T.; Yamaguchi, S.; Waring, A. J.; Lehrer, R. I.; Hong, M. *Biophys. J.* **2003**, *85*, 2363–2373.
(29) Wiener, M. C.; White, S. H. *Biophys. J.* **1992**, *61*, 434–447.

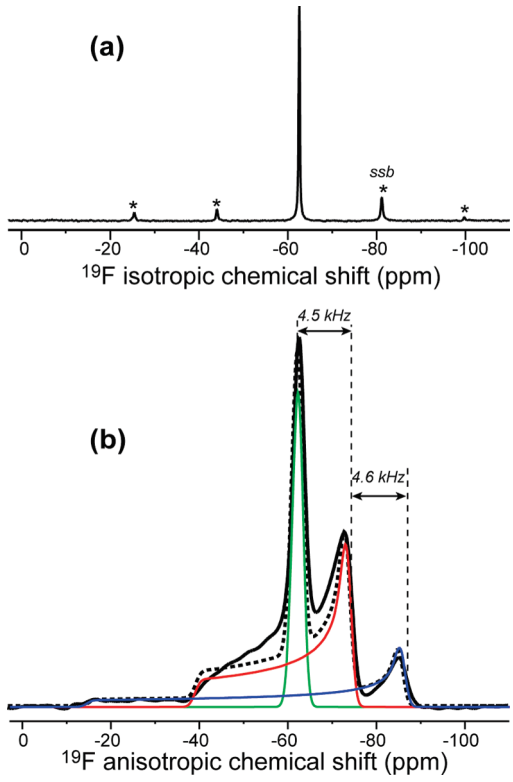

Figure 4. ^{19}F spectrum of PMX30016 in unoriented DMPC/DMPG (3:1) bilayers. (a) MAS spectrum. (b) Static spectrum (black line). Three simulated powder patterns corresponding to $\omega_{CSA} - \omega_D$ (green), ω_{CSA} (red), and $\omega_{CSA} + \omega_D$ (blue), at 1:2:1 area ratios are shown. The sum of the three simulated patterns is shown as a dashed line. A line broadening of 10 ppm was used for each subspectrum. The 90° edges of the triplet are spaced by a ^{19}F−^{19}F dipolar coupling of 4.5 kHz.

membrane surface.[27] The difference between the two spectra also clearly demonstrates that Mn^{2+} is not freely permeable to the inside of the vesicle, thus ruling out the possibility that the arylamide forms large stable pores.

To obtain more quantitative depth information, we compared the PRE effects of all lipid ^{13}C signals in the one-sided and two-sided Mn^{2+} samples with the ^{19}F PRE of PMX30016 (Figure 3b). The lipid signals show the expected trend of increasing residual intensity (weaker PRE) with increasing distance from the membrane surface, and the two-sided Mn^{2+} samples have lower residual intensities than the one-sided Mn^{2+} sample. The ^{19}F intensities are comparable to that of the headgroup carbons for each sample, indicating that PMX30016 is shallowly inserted into the membrane−water interface, between the phosphate groups and the glycerol backbone region.

Orientation and Uniaxial Rotation of PMX30016 in Lipid Bilayers. The ^{19}F MAS spectrum of PMX30016 in DMPC/DMPG bilayers (Figure 4a) shows only a single ^{19}F peak (−62.6 ppm), indicating that the two trifluoromethyl groups have the same chemical environment in lipid membranes. Under the static conditions, the ^{19}F spectrum shows a triplet powder pattern with three distinct 90° edges at −62.6, −73.4, and −85.4 ppm (Figure 4b). This triplet pattern is well-known for CF_3 groups as resulting from ^{19}F−^{19}F dipolar splitting of each ^{19}F by the two other fluorines in the trifluoromethyl group and has been explored extensively for orientation measurements of membrane peptides.[19,20] The three components of the triplet correspond to the unperturbed chemical shift spectrum and the sum and difference of the anisotropic dipolar and chemical shift frequencies: $\omega_{CSA} - \omega_D$, ω_{CSA}, and $\omega_{CSA} + \omega_D$. Analogous to the C−H J-splitting of a CH_2 group, the integrated intensities of the three subspectra have the ratio 1:2:1. Figure 4b shows that the central component of the PMX30016 triplet has a uniaxial line shape ($\eta = 0$), indicating that the molecule undergoes fast uniaxial rotation around the bilayer normal. This motion averages both the ^{19}F−^{19}F dipolar coupling and the ^{19}F CSA to be uniaxial and collinear with the bilayer normal. As a result, the sum and difference spectra are particularly simple: they have $\eta = 0$ line shapes and anisotropy parameters of $\bar{\delta}_{CSA} + \bar{\delta}_D$ and $\bar{\delta}_{CSA} - \bar{\delta}_D$. Since the central 90° edge of the triplet (−73.4 ppm) is 4.4 kHz from the two other 90° edges, the motionally averaged ^{19}F−^{19}F dipolar coupling constant $\bar{\delta}_D$ is 4.4 kHz. Figure 4b shows a simulated ^{19}F spectrum based on a 1:2:1 superposition of three $\eta = 0$ powder patterns with motionally averaged anisotropy parameters of 0.5, 23.6, and 46.7 ppm, respectively. The simulation has excellent agreement with the experimental spectrum, confirming the nature of the triplet.

To better resolve the ^{19}F−^{19}F dipolar coupling from the ^{19}F CSA, we implemented a 2D dipolar chemical-shift (DIPSHIFT) correlation experiment where a 180° pulse in the middle of the t_1 evolution period encodes pure ^{19}F−^{19}F dipolar coupling in the indirect dimension and correlates it with the mixed CSA-dipolar spectrum in the direct dimension (Figure 5a). Although the directly detected dimension is not a pure chemical shift spectrum, for simplicity we use the terminology of homonuclear DIPSHIFT to refer to this experiment. Pure ^{19}F dipolar spectra have been previously extracted mainly using the 1D Carr−Purcell−Meiboom−Gill (CPMG) experiment,[30,31] where the ^{19}F signals were detected in the windows of long multiple-pulse trains.[19,24,32] Compared to the multiple-pulse experiment, this 2D Hahn-echo based homonuclear DIPSHIFT experiment has the benefits of a lower radio frequency duty cycle and a simpler signal acquisition method, since windowed detection entails scaling of the spectral width and is sensitive to the cumulative effects of pulse imperfections.

We first applied the static 2D homonuclear DIPSHIFT experiment to PMX30016 in magnetically aligned DMPC/6-O-PC bicelles. The alignment axis of the bicelle is perpendicular to the magnetic field, thus scaling all measured couplings by −0.5 (Figure 5b). The 2D spectrum shows the expected correlation of the triplet pattern in the ω_2 dimension with ^{19}F−^{19}F dipolar coupling in the ω_1 dimension. Both the most downfield (−61.5 ppm) and the most upfield (−75.3 ppm) ^{19}F peaks exhibit a doublet splitting of 5.2 kHz, as expected because these two ^{19}F peaks correlate with dipolar couplings with the same magnitude, $\bar{\delta}_{CSA} - \bar{\delta}_D$ and $\bar{\delta}_{CSA} + \bar{\delta}_D$, and the dipolar spectrum is sign-insensitive. Also as expected, the central ^{19}F peak (−68.5 ppm) does not exhibit a splitting because it corresponds to the unperturbed CSA, $\bar{\delta}_{CSA}$. The dipolar coupling constant of interest is half the splitting, which is thus 2.6 kHz.

We now consider the orientation dependence of the motionally averaged ^{19}F−^{19}F dipolar coupling of the CF_3 group. For two ^{19}F spins separated by 2.09 Å as in a CF_3 group, the homonuclear ^{19}F−^{19}F dipolar coupling in the absence of motion is 17.6 kHz. The three-site jumps of the CF_3 scales the coupling by a factor of $(3\cos^2 90 - 1)/2 = -0.5$ due to the 90° angle between each F−F vector and the C−CF_3 axis. Thus, the ^{19}F−^{19}F coupling of a rotating CF_3 group without any *other*

(30) Carr, H. Y.; Purcell, E. M. *Phys. Rev.* **1954**, *94*, 630–638.
(31) Meiboom, S.; Gill, D. *Rev. Sci. Instrum.* **1958**, *29*, 688–691.
(32) Grage, S. L.; Ulrich, A. S. *J. Magn. Reson.* **1999**, 98–106.

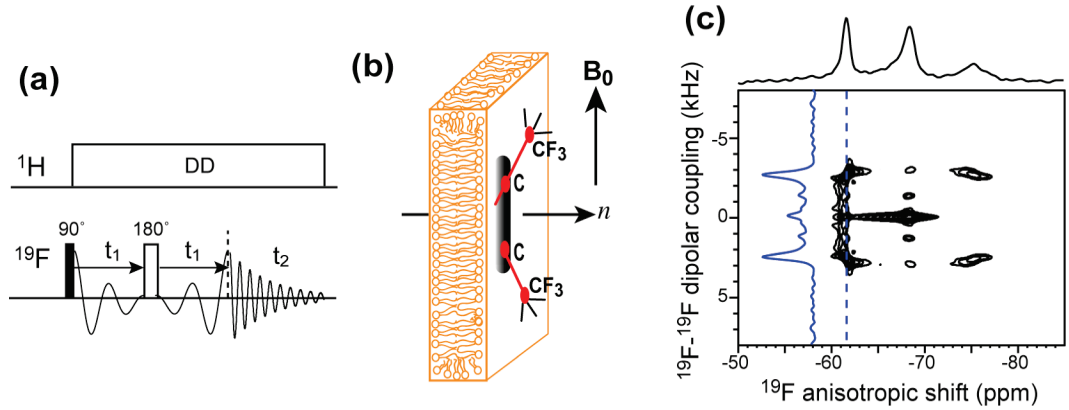

Figure 5. Orientation determination of PMX30016 in neutral lipid bilayers. (a) Static 2D ^{19}F dipolar chemical-shift correlation pulse sequence for measuring ^{19}F−^{19}F dipolar couplings. (b) Geometry of magnetically oriented bicelles containing PMX30016. (c) Static 2D ^{19}F homonuclear DIPSHIFT spectrum of PMX30016 in aligned DMPC/6-O-PC bicelles. The dipolar cross section at −62 ppm is shown as a blue trace.

motion is 8.8 kHz. If the C−CF$_3$ axis undergoes rotation around the bilayer normal, then the dipolar couplings will be scaled by an orientation-dependent factor.

$$S_{CC,n} = (3\cos^2\theta_{CC,n} - 1)/2$$

All lipids and peptides in aligned bicelles rotate around the bicelle normal, which is perpendicular to the magnetic field in our case. The bicelle normal usually exhibits a small degree of wobbling, as described by an order parameter $S_{bicelle}$. These two effects further reduce the dipolar coupling, so that the total measured ^{19}F−^{19}F coupling is:

$$\bar{\omega}_D^{CF_3,bicelle} = 8.8\text{ kHz} \times |(-0.5)|_{bicelle} \times S_{bicelle} \times S_{CC,n} = 3.9 \times S_{CC,n}\text{ kHz} \quad (1)$$

In the above equation we have used a $S_{bicelle}$ value of 0.89, which was directly measured from the ^{31}P spectrum according to

$$S_{bicelle} = (\delta_{obs} - \delta_{iso})/(\delta_{90^\circ} - \delta_{iso}) \quad (2)$$

where $\delta_{iso} = -0.9$ ppm, $\delta_{90^\circ} = -14.9$ ppm, and $\delta_{obs} = -13.3$ ppm. This $S_{bicelle}$ value is consistent with the literature range of 0.75 − 0.94, which depends on the q ratio, the hydration level, and temperature of the bicelle.[26,33]

In unoriented membranes where the molecule of interest undergoes uniaxial diffusion, the observed ^{19}F−^{19}F dipolar coupling constant is larger due to the lack of two scaling factors:

$$\bar{\delta}_D^{CF_3,powder} = 8.8 \times S_{CC,n}\text{ kHz} \quad (3)$$

Equations 1 and 3 show that the ^{19}F−^{19}F dipolar coupling of the CF$_3$ group ultimately depends only on the angle between the C−CF$_3$ bond and the bilayer normal. Since the C−CF$_3$ bond is rigidly held to the rest of the arylamide ring plane, this vector orientation reveals the orientation of the rigid molecular plane with respect to the membrane normal. Thus, simulation of the ^{19}F−^{19}F dipolar coupling can yield the orientation of PMX30016 in the lipid bilayer.

Figure 6b shows the calculated ^{19}F−^{19}F dipolar couplings as a function of the tilt angle and rotation angle of the arylamide with respect to the bilayer normal. A tilt angle of 0° and 90°

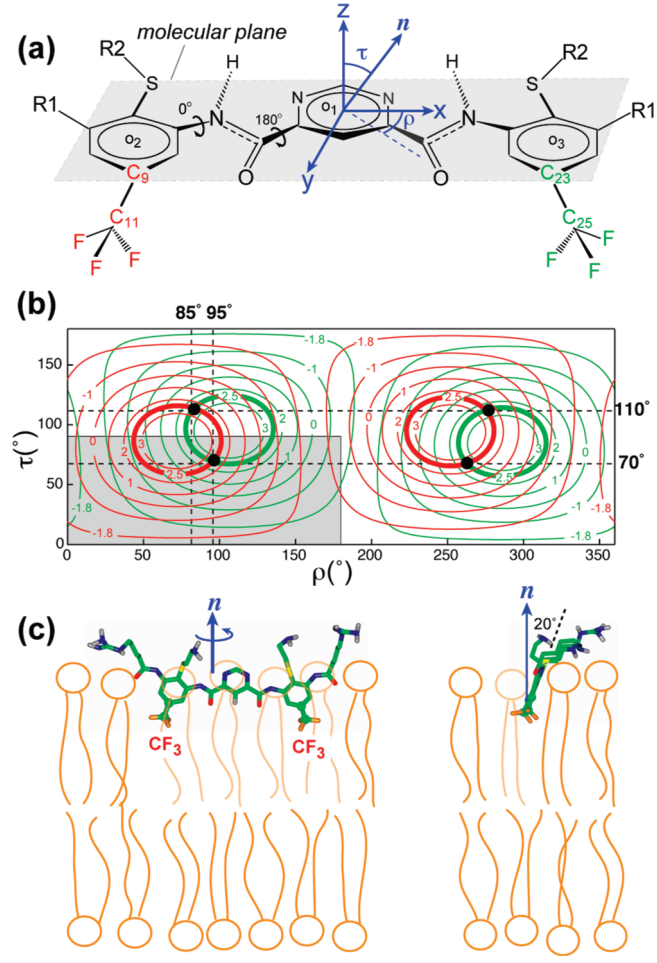

Figure 6. Extraction of the orientation of PMX30016 in neutral DMPC/6-O-PC bicelles. (a) Definitions of the molecular coordinate system and (τ, ρ) angles. (b) Calculated ^{19}F−^{19}F dipolar couplings as a function of (τ, ρ) for the CF$_3$ groups associated with the C9−C11 bond (red) and the C23−C25 bond (green). Contour lines for the measured value of 2.6 kHz are bolded. The best-fit (τ, ρ) = (70°, 95°) and its degenerate solutions are indicated as black dots. The nondegenerate region of the orientation plot is shown in gray. (c) Front (left) and side (right) views of the orientation of PMX30016 in DMPC bilayers. The plane of PMX30016 is tilted by 20° from the bilayer normal, which corresponds to τ = 70°.

means, respectively, that the normal of the molecular plane is parallel and perpendicular to the bilayer normal. A rotation angle of 0° and 90° corresponds to the long molecular axis being

(33) Yamamoto, K.; Soong, R.; Ramamoorthy, A. *Langmuir* **2009**, *25*, 7012–7018.

parallel and perpendicular to the bilayer normal, respectively. The observation of only one ^{19}F−^{19}F dipolar coupling in the static spectrum indicates that the two C−CF_3 bonds have the same orientation with respect to the bilayer normal. The calculated dipolar couplings of the two CF_3 groups are shown in red and green contour lines, and the contour lines corresponding to the observed 2.6 kHz coupling are thickened. Since both CF_3 groups exhibit the same coupling, only a single solution of (τ, ρ) = (70°, 95°) was identified within the unique quadrant of 0°−180° for ρ and 0°−90° for τ. All other solutions such as (τ, ρ) = (110°, 85°) are degenerate. Figure 6c shows the (τ = 70°, ρ = 95°) orientation of PMX30016 in the DMPC bilayer. The molecular plane is almost perpendicular to the bilayer plane, reflecting the tilt angle, while the long axis of the molecule is nearly parallel to the bilayer surface, reflecting the rotation angle. This orientation corresponds to a knife-like insertion of the arylamide into the membrane, with the aromatic plane only 20° from the vertical bilayer normal.

To determine whether the orientation is affected by the presence of negatively charged lipids, we measured the 2D ^{19}F DIPSHIFT spectrum of PMX30016 in unoriented DMPC/DMPG bilayers. Figure 7a shows a similar triplet pattern in the direct dimension, but it is now correlated with a larger dipolar splitting of 8.6 kHz due to the absence of two bicelle scaling factors (eq 3). The dipolar coupling constant of 4.35 kHz was calculated to yield a unique orientation solution of (τ = 60°, ρ = 99°) (Figure 7b), indicating that now the molecular plane is moderately more tilted from the bilayer normal (30°) than the case in the neutral DMPC bilayer, but the long molecular axis remains largely parallel to the membrane plane. Overall, the knife-like insertion motif is maintained, as shown in Figure 7c.

Discussion

The above solid-state NMR data provide the most comprehensive information to date about the lipid interaction, depth of insertion, orientation, and dynamics of an arylamide oligomer. We first discuss the membrane topology of this arylamide foldamer. In both neutral DMPC bilayers and anionic DMPC/DMPG bilayers, the long molecular backbone lies parallel to the bilayer surface, as reflected by $\rho \approx 90°$. Our ^{19}F NMR method allows precise measurement of the orientation of the phenyl rings of the arylamide molecule. We did not measure the orientation of the central pyrimidyl ring, but previous studies showed it to be constrained to lie coplanar with the phenyl rings through the formation of an extended hydrogen-bonded network (Figure 1).[9] The two phenyl groups are oriented with their rigid aryl planes nearly perpendicular to the membrane surface (τ = 60°, 70°). The phenyl ring's deviation from perpendicularity is 20° for the neutral bilayer and 30° for the anionic bilayer. This orientation resembles a knife cutting into the bilayer, which would be logical because it matches the amphiphilic structure of the arylamide with the amphiphilic structure of the lipid bilayer, by pointing the basic guanidinium and the amino-ethyl thioether substituents to the aqueous surface of the membrane while pointing the hydrophobic groups toward the lipid chains. The parallel orientation of the long molecular axis with the membrane plane satisfies the 2-fold symmetry of the molecule and maintains the same intermolecular potentials for the two sides of the pyrimidine ring, which are chemically identical. The moderate difference in the tilt angle between the neutral and anionic membranes can be understood by the fact that the less vertical molecular plane enables the positively charged guanidinium groups to interact more strongly with the negatively

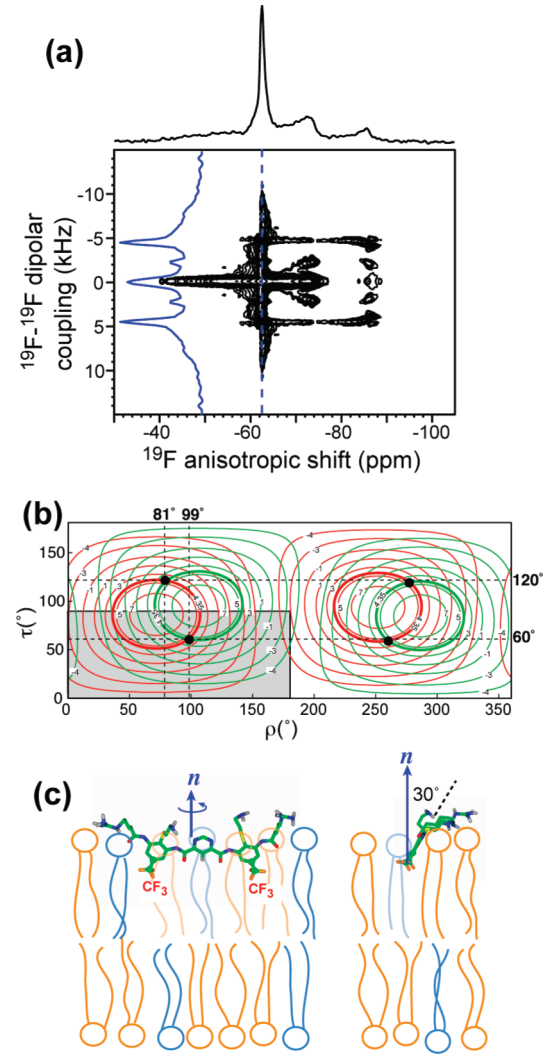

Figure 7. Orientation of PMX30016 in unoriented DMPC/DMPG membranes. (a) 2D ^{19}F homonuclear DIPSHIFT spectrum of PMX30016 in DMPC/DMPG (3:1) membranes. (b) Calculated ^{19}F−^{19}F dipolar couplings as a function of (τ, ρ) angles. The intercepts of the two CF_3 groups' couplings at 4.35 kHz give the best-fit orientation, which is (τ, ρ) = (60°, 99°). The nondegenerate region of the orientation plot is shown in gray. (c) Best-fit orientation of PMX30016 in anionic lipid membranes.

charged DMPG headgroups on the membrane surface (Figure 7c). In other words, competition between water and the negative charge density of the membrane surface may cause a small modulation of the tilt angle of the arylamide plane.

The knife-like orientation of PMX30016 obtained here is in excellent agreement with the results of SFG vibrational spectra of an analogous arylamide.[12] There, analysis of the symmetric and asymmetric stretching modes of *tert*-butyl side chains adsorbed onto DPPG bilayers concluded an angle of 0°−35° for the 3-fold axis of the *tert*-butyl. This orientation, while limiting in nature, is consistent with the ^{19}F NMR result for the DMPC/DMPG-bound PMX30016, where the molecular plane is 30° from the bilayer normal (Figure 7c). Since the two arylamide molecules differ in their basic side chains and the hydrophobic functional groups, the similarity of the results indicates that the facial amphiphilicity and restrained backbone structure of the molecules are sufficient to determine their orientations. The ^{19}F NMR constraints obtained here have higher angular resolution and more complete information than the SFG results, since as long as the arylamide plane is not exactly

perpendicular to the bilayer plane, a second angle defining the long axis direction is necessary to fully describe the molecular orientation.

Paramagnetic relaxation enhancement data indicate that the knife-like arylamide inserts only shallowly into the membrane, just below the phosphate headgroups and not reaching into the acyl chain region (Figure 3). The shallow depth was obtained at a drug/lipid molar ratio of 1:15, at which the arylamide was already distributed into both leaflets of the bilayer. Direct comparisons of the drug/lipid molar ratios in the hydrated pastes of the solid-state NMR samples versus the aqueous solutions of antimicrobial assays are fraught with uncertainties. Nevertheless, we believe at higher arylamide concentrations the equilibrium structure is unlikely to be a deeper transmembrane insertion, and the mechanism of action of the arylamide should be considered in the context of the observed shallow depth and knife-like orientation. This topology should be combined with the fact that the drug undergoes fast uniaxial diffusion at rates greater than 10^5 s^{-1}. Thus, the rigid arylamide knife is by no means static but spins around the membrane normal with its full extended length, which has the potential to perturb and destabilize a large area of the membrane.

The topology and dynamics of PMX30016 in the lipid bilayer are inconsistent with the three main classical antimicrobial structural models, namely, the barrel-stave,[34,35] the toroidal pore,[36,37] and the carpet models.[38] The arylamide foldamer is not transmembrane and does not cause lipid orientational disorders of the toroidal type. The knife-like topology is also distinct from the carpet model, since the arylamide does not aggregate into extended immobile assemblies.

One of the most intriguing aspects of the arylamide interaction with the lipid membrane is the increased ^{31}P CSA and the nearly complete absence of orientational disorder as the concentration of the foldamer increases. These features indicate that the doubly charged molecule influences the headgroup conformation of the phospholipids without causing large-scale orientation disruption of the bilayer. It is well-known that the polar lipid headgroups act as molecular electrometers to membrane surface charges.[39] The addition of positively charged metal ions, hydrophobic ions, amphiphiles, and peptides increases the magnitude of the ^{31}P CSA and the ^{2}H quadrupolar coupling of the headgroup β-CD_2 but decreases the ^{2}H coupling of the α-CD_2.[39−42] The addition of negatively charged species to the membrane surface creates the opposite effects. Based on analysis of the ^{31}P chemical shift tensor and ^{2}H quadrupolar couplings, it was proposed that cationic species change the lipid headgroup conformation such that the N^+ end of the $^-P-N^+$ dipole moves toward the water phase. The PMX30016-induced ^{31}P CSA increase is consistent with this electrometer effect both qualitatively and quantitatively. A cationic amphiphile, sodium dialkyl phosphate, was found to increase the ^{31}P CSA of POPC lipids by 8 ppm at 20 mol% amphiphile.[40] Similarly, at 8 mol % arylamide, which corresponds to a 16 mol% positive charge density, the ^{31}P CSA span of the POPE/POPG membrane increased by 7.8 ppm (Figure 2).

The ^{19}F NMR results of the arylamide and the ^{31}P NMR spectra of the lipids, taken together, suggest that the antimicrobial arylamide disrupts the membrane barrier function of microbial cells primarily by altering the membrane electric potential profile. While the spinning molecular knife would certainly perturb lipid packing on the molecular level, it appears to do so only transiently and leaves no long-lasting physical damage behind. The lack of permanent membrane disorder by PMX30016, manifested by the ^{31}P spectra, is in sharp contrast to many other antimicrobial peptides such as PG-1[18,43] and magainin.[44] The absence of permanent disruption is more akin to tachyplesin, which, interestingly, also exhibits fast uniaxial rotation with an in-plane orientation.[17,45] Instead, the spinning arylamide knife, with its positively charged guanidinium groups, significantly alters the lipid headgroup conformation, an effect that is absent for tachyplesins. We propose that this perturbation of the lipid headgroup conformation changes the membrane surface potential and eventually leads to membrane permeabilization. Possible interaction between the arylamide and protein components of bacterial membranes may also be involved at that stage.

At higher drug concentrations than those used in this study, it is possible that the spinning arylamide may increasingly cause more pronounced physical disruption of the membrane, so that a balance between the two effects−perturbation of the membrane potential versus the physical disruption−may be responsible for bacterial killing. Such a mixed mechanistic scenario has been suggested before for analogous antimicrobial arylamides based on different concentrations and kinetics of membrane permeabilization and bacteria killing.[10] The possibility of a mixture of mechanistic modes has also been gleaned for some antimicrobial peptides. For example, magainin showed clear signs of physical disruption of lipid membranes based on ^{31}P NMR spectra,[44] but it also dissipates the electrical potential across lipid membranes and has been proposed to kill bacteria by decreasing the membrane potential and interfering with free-energy transduction in microbial cells.[46]

The present study illustrates the robustness and utility of ^{19}F solid-state NMR for elucidating the topology and dynamics of pharmaceutical compounds. The high sensitivity and lack of background of ^{19}F spins, combined with the large chemical shift anisotropy and $^{19}F-^{19}F$ dipolar couplings, make ^{19}F NMR exquisitely sensitive to molecular orientation and dynamics. The simple 2D ^{19}F homonuclear DIPSHIFT experiment, while analogous to several other NMR techniques,[47−49] has not been employed before for determining orientation-dependent dipolar

(34) Baumann, G.; Mueller, P. *J. Supramol. Struct.* **1974**, *2*, 538–557.
(35) He, K.; Ludtke, S. J.; Worcester, D. L.; Huang, H. W. *Biophys. J.* **1996**, *70*, 2659–2666.
(36) Ludtke, S. J.; He, K.; Heller, W. T.; Harroun, T. A.; Yang, L.; Huang, H. W. *Biochemistry* **1996**, *35*, 13723–13728.
(37) Matsuzaki, K.; Murase, O.; Fujii, N.; Miyajima, K. *Biochemistry* **1996**, *35*, 11361–11368.
(38) Pouny, Y.; Rapaport, D.; Mor, A.; Nicolas, P.; Shai, Y. *Biochemistry* **1992**, *31*, 12416–12423.
(39) Seelig, J.; MacDonald, P. M.; Scherer, P. G. *Biochemistry* **1987**, *26*, 7535–7541.
(40) Scherer, P. G.; Seelig, J. *Biochemistry* **1989**, *28*, 7720–7728.
(41) MacDonald, P. M.; Leisen, J.; Marassi, F. M. *Biochemistry* **1991**, *30*, 3558–3566.
(42) Ziegler, A.; Blatter, X. L.; Seelig, A.; Seelig, J. *Biochemistry* **2003**, *42*, 9185–9194.
(43) Yamaguchi, S.; Waring, A.; Hong, T.; Lehrer, R.; Hong, M. *Biochemistry* **2002**, *41*, 9852–9862.
(44) Bechinger, B. *Biochim. Biophys. Acta* **2005**, *1712*, 101–108.
(45) Doherty, T.; Waring, A. J.; Hong, M. *Biochemistry* **2008**, *47*, 1105–1116.
(46) Westerhoff, H. V.; Juretić, D.; Hendler, R. W.; Zasloff, M. *Proc. Natl. Acad. Sci. U.S.A.* **1989**, *86*, 6597–6601.
(47) Bennett, A. E.; Becerra, L. R.; Griffin, R. G. *J. Chem. Phys.* **1994**, *100*, 812–814.
(48) Wu, C. H.; Ramamoorthy, A.; Opella, S. J. *J. Magn. Reson.* **1994**, *109*, 270–272.
(49) Munowitz, M. G.; Griffin, R. G.; Bodenhausen, G.; Huang, T. H. *J. Am. Chem. Soc.* **1981**, *103*, 2529–2533.

couplings and promises to facilitate high-resolution structural analysis of CF_3-containing pharmaceutical compounds.

Conclusion

The orientation, depth of insertion, mobility, and lipid interaction of an antimicrobial arylamide has been determined using ^{19}F and ^{31}P solid-state NMR. The arylamide inserts into the lipid membrane just below the headgroups with the molecular plane nearly perpendicular to the bilayer surface and the long axis parallel to the bilayer. In this knife-like manner, the molecule undergoes fast uniaxial rotation around the bilayer normal. Interestingly, this spinning molecular knife does not directly cause permanent damage to the lamellar integrity of the lipid bilayer but rather changes the lipid headgroup conformation, specifically, the P−N dipole orientation, through interaction of the positively charged guanidinium ions with the lipid phosphate groups. This conformational change, manifested as ^{31}P chemical shift increases, was detected in all negatively charged lipid membranes studied here. We propose that the antimicrobial arylamide destroys the barrier function of the microbial cell membrane mainly by altering its electrical potential, and the spinning molecular knife may further create transient defects in the membrane.

Acknowledgment. This work is funded by NIH Grants GM66976 to M.H., AI75866 to W.F.D., and UL1RR024134 from the National Center For Research Resources.

JA103658H